communications earth & environment

Article

A Nature Portfolio journal

https://doi.org/10.1038/s43247-025-02801-4

Prolonged drought on Rapa Nui during the decline of megalithic monument construction

Redmond Stein [1] ✉, Lorelei Curtin[2], Nicholas L. Balascio[3], Raymond S. Bradley[4], Dorothy M. Peteet[1,5], Rafael Rapu[6], Valentí Rull [7,8], Andrea Seelenfreund [9] & William J. D'Andrea [1] ✉

Beginning in the 13th century, Polynesian settlers on the island of Rapa Nui engaged in megalithic monument construction, crafting hundreds of *ahu* platforms and *moai* statues from volcanic bedrock. The decline of this tradition centuries later, coincident with land-use changes and the emergence of new ritual practices on the island, has intrigued archaeologists for decades. Here, we present evidence for a transition to persistent drought conditions on Rapa Nui beginning in the mid 16th century, based on two independent reconstructions of hydrogen isotopes in rainfall inferred from hydrogen isotopes of leaf waxes preserved in wetland sediments. Consistent with observational data and model simulations, we interpret more negative hydrogen isotopes in precipitation to reflect an increase in the frequency of large storms and total rainfall amount over Rapa Nui. We show that 16th–17th century changes in human geography on Rapa Nui coincided with a sustained, multi-century decrease in annual precipitation of ~600–800 mm, which is of greater magnitude than the drying observed in recent decades.

Changes in hydroclimate have been linked to major socio-political transformations globally, particularly in arid regions where freshwater availability depends strongly on precipitation[1–6]. On Rapa Nui (27.15°S, 109.4°W), surface freshwater resources are extremely limited. Despite receiving a moderate amount of rainfall (~1100 mm), local bedrock is composed of jointed basalt flows, allowing rainwater to rapidly drain through the subsurface[7–10]. The sole freshwater surface reservoirs on Rapa Nui are Rano Raraku lake, Rano Kao lake, and Rano Aroi wetland, all located within dormant volcanic craters (Fig. 1). Rano Raraku is prone to desiccation[11,12], however, and in recent years both Rano Aroi and Rano Raraku have dried completely. Understanding how precipitation varied in the past on Rapa Nui therefore provides critical context for understanding its human geography, including the growth and decline of megalithic architecture, as well as contemporaneous shifts in social hierarchies and spatial organization.

Most recent estimates for Polynesian arrival on Rapa Nui fall between 1200 and 1280 CE[11,13–16]. Soon after settlement, the Rapanui began a centuries-long tradition of building massive *moai* statues and ceremonial *ahu* platforms (Fig. 1), with construction likely accelerating between 1350 and 1450 CE[14,17]. Society at this time was organized into a conical clan structure, wherein the most power was held by those who could trace their ancestral lineage back to the original Polynesian settlers[18]. *Moai* statues themselves served as deified representations of ancestors, and their production by the hundreds in Rano Raraku quarry served as an organizing principle for Rapanui society[19–22].

This mode of social organization and its associated geographical, political, and ritual manifestations likely began to shift in the late 16th to early 17th century, prior to European contact (see Rull & Stevenson, 2022 for a thorough review). During this time period, the construction of *ahu* platforms declined[14,17] along with the prestige of the previous religious political order, and the tradition known as *Tangata Manu* emerged, wherein chiefly power was attained through ritual athletic competition[23–25]. The spiritual center of the Rapanui shifted in tandem, moving from Rano Raraku crater lake, used as a quarry for *moai* construction, to Rano Kao (Fig. 1)[26]. While Rano Kao was in use prior to the 17th century[27], radiocarbon and obsidian hydration dates suggest that activity increased significantly at Orongo village and Mata Ngarau (on the crater rim) between 1600 and 1650 CE, including the construction of extensive stone hut complexes[23]. An increase in fire

[1]Lamont-Doherty Earth Observatory, Palisades, NY, USA. [2]Bucknell University, Lewisburg, PA, USA. [3]Bates College, Lewiston, ME, USA. [4]University of Massachusetts, Amherst, MA, USA. [5]NASA Goddard Institute for Space Studies, New York, NY, USA. [6]Universidad Católica del Norte, Antofagasta, Chile. [7]Botanic Institute of Barcelona, Spanish National Research Council, Barcelona, Spain. [8]Institut Català de Paleontologia Miquel Crusafont, Universitat Autònoma de Barcelona, Cerdanyola del Vallès, Spain. [9]Universidad Academia de Humanismo Cristiano, Santiago, Chile. ✉e-mail: redstein@ldeo.columbia.edu; dandrea@ldeo.columbia.edu

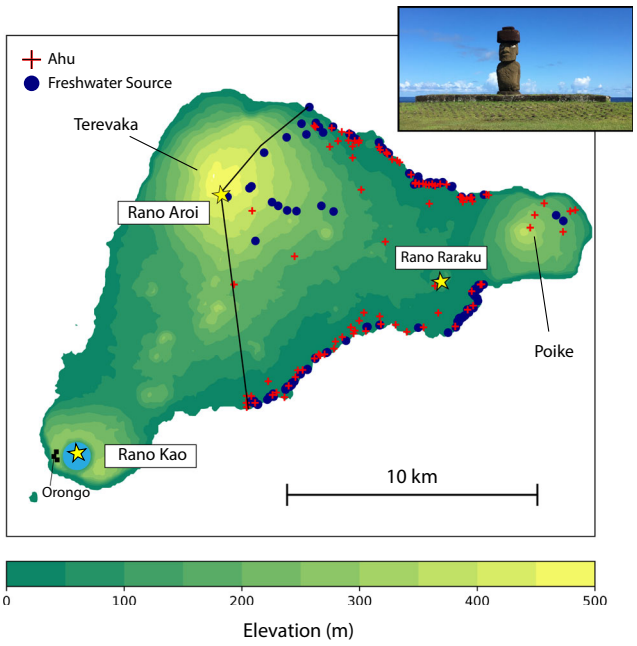

Fig. 1 | Elevation map of Rapa Nui with freshwater sources highlighted. Digital elevation model of Rapa Nui (27.15°S, 109.4°W), from NOAA's National Center for Environmental Information. Permanent lakes and wetlands, including Rano Kao, Rano Raraku, and Rano Aroi, are starred and labelled. Other freshwater sources, including springs, ponds, caves with seeping groundwater, *puna*, and coastal groundwater discharge, are marked by navy circles. These sites were identified and mapped by DiNapoli et al.[59] within the eastern sector of the island, bounded by solid black lines[59]. The locations of *Ahu* platforms within this study area are marked with red crosses. A photo of an *ahu* platform and single *moai* statue is shown in the upper right corner.

indicators and fecal indicators (coprophilous fungal spores) in wetland sediment cores from Rano Kao also suggest an interval of human occupation at Rano Kao from ~1550 CE onwards, with an increase in activity ~1600 CE[28]. Obsidian hydration dating further places the abandonment[29] and/or decreased usage[30] of certain agricultural fields in the early 17th century. Whether or not the construction of new *ahu* and *moai* ceased completely during this time of transition is still a point of debate. Previous visual inspection of radiocarbon and obsidian hydration dates from Rapa Nui have led researchers to argue for limited construction events after 1500–1600 CE[31], or even a destruction of *ahu* beginning ca. 1600 CE[17]. Recent Bayesian models suggest that *ahu* construction peaked between 1350 and 1450 CE and slowly declined from 1550 CE through the 18th century[14].

An abundance of evidence now makes clear that population size on Rapa Nui was stable through the 16th-17th century and did not decline prior to the devastation wrought by European and Peruvian traders and enslavers over a century later[32–36]. Highly popularized narratives of island-wide demographic collapse driven by resource depletion (or 'ecocide') during this time period[37] have no concrete basis in the archeological record.

Drought conditions beginning in the middle of the 16th century have previously been proposed based on a sedimentary depositional hiatus in Rano Raraku[12] and elemental geochemical analyses from Rano Aroi sediment[38]. Water scarcity[12,23,29,38,39], nutrient depletion of soils due to intensive agricultural use[30], and island deforestation[20,37] have been invoked to explain the apparent cultural transition and spatial reorganization of the 16th–17th centuries. To understand how freshwater availability varied through this transformative period on Rapa Nui, we measured the hydrogen isotope composition (δ^2H) of leaf waxes (*n*-alkanoic acids) preserved in sediments from Rano Aroi wetland and Rano Kao lake (see Methods). We use these records to assess the timing and magnitude of changes in rainfall over the island and to infer associated changes in Southeast Pacific atmospheric circulation. Importantly, these δ^2H measurements provide a continuous and direct, proxy-based record of hydroclimate that spans the entirety of the human interval on Rapa Nui prior to European contact.

Results and Discussion

Modern δ^2H_{precip} values on Rapa Nui covary with precipitation amount

Rapa Nui is located in the remote southeast Pacific Ocean, at the juncture of three major atmospheric systems: the South Pacific Anticyclone (SPA), the South Pacific Convergence Zone (SPCZ), and the midlatitude westerlies (Supplementary Fig. 1). Today the island receives ~1100 mm of rainfall per year on average, but interannual precipitation budgets are highly variable[10]. Total annual precipitation is determined almost entirely by the frequency of large storms (delivering > 20 mm of rainfall, after ref. 40) that pass over the island, which explains 92% of the observed variance in total rainfall amount[40]. Seasonal changes in storm frequency over Rapa Nui are explained by the seasonality of the SPA. In austral summer, the SPA strengthens and expands, blocking large storm systems associated with the midlatitude westerlies from passing over the island[40,41]. Recent work by Steiger et al.[40] shows that SPA position explains 21% of the observed variance in annual rainfall from 1955 to present, and the remaining variance cannot be explained by any mode of synoptic climate variability. Some authors have argued that La Niña conditions correspond with rainfall deficits over Rapa Nui[42], however, other recent analyses have shown that this relationship is not statistically significant for the instrumental period[10].

We explored the relationship between δ^2H_{precip} and precipitation amount over Rapa Nui using monthly measurements of stable isotopes in rainfall, available from 1991 to 2018 ($n = 317$) through the Global Network of Isotopes in Precipitation (GNIP)[43]. Annual precipitation-weighted δ^2H_{precip} in this dataset has a significant negative correlation with mean annual precipitation ($R = -0.52$, $p = 0.008$) (Fig. 2A) and with the annual frequency of large storms, ($R = -0.57$ and $p = 0.003$) (Fig. 2B), while showing an insignificant relationship to annual mean temperature and vapor pressure (Supplementary Fig. 2). The equation describing the relationship between rainfall amount and δ^2H_{precip} values is:

$$\delta^2H_{Annual\ precip} = \frac{-1.4‰ VSMOW}{100mm} X_{MAP} + 7.9‰ \quad (1)$$

where X_{MAP} is equal to the mean annual precipitation in millimeters.

On a monthly basis, δ^2H_{precip} values show a weak, but significant correlation with rainfall amount ($R = -0.32$, $p < 0.01$). Months with fewer large storms have more positive δ^2H_{precip} values on average. With increasing large storm frequency, monthly δ^2H_{precip} values decrease and converge towards a mean of approximately −20‰ (VSMOW-SLAP), and the range of observed δ^2H_{precip} values decreases in tandem (Supplementary Fig. 3). This may indicate that precipitation associated with large storm systems has a consistently more negative isotopic signature, while precipitation associated with smaller rainfall events may have more variable isotopic composition, attributable to changing source region, relative humidity during rainout, or varying degrees of Rayleigh distillation[44]. On longer timescales (1871-2011), ECHAM5-wiso model simulations suggest that monthly δ^2H_{precip} values over Rapa Nui and the surrounding region have a significant negative correlation with regional precipitation amount (Fig. 2C), and a significant positive relationship with easterly wind velocity and sea level pressure associated with SPA circulation (Supplementary Fig. 4)[45]. Although the ECHAM5-wiso data do not accurately represent observed δ^2H_{precip} values over Rapa Nui (e.g., modeled δ^2H_{precip} values are consistently more negative and show less month-to-month variability than measured δ^2H_{precip} on Rapa Nui), the model offers mechanistic insight into the underlying processes that affect isotopes in precipitation.

δ^2H_{wax} in Rano Aroi and Rano Kao reflects δ^2H_{precip}

Long chain *n*-alkanoic acids record the isotopic composition of amount-weighted source water during their growing season[46]. On Rapa Nui, where

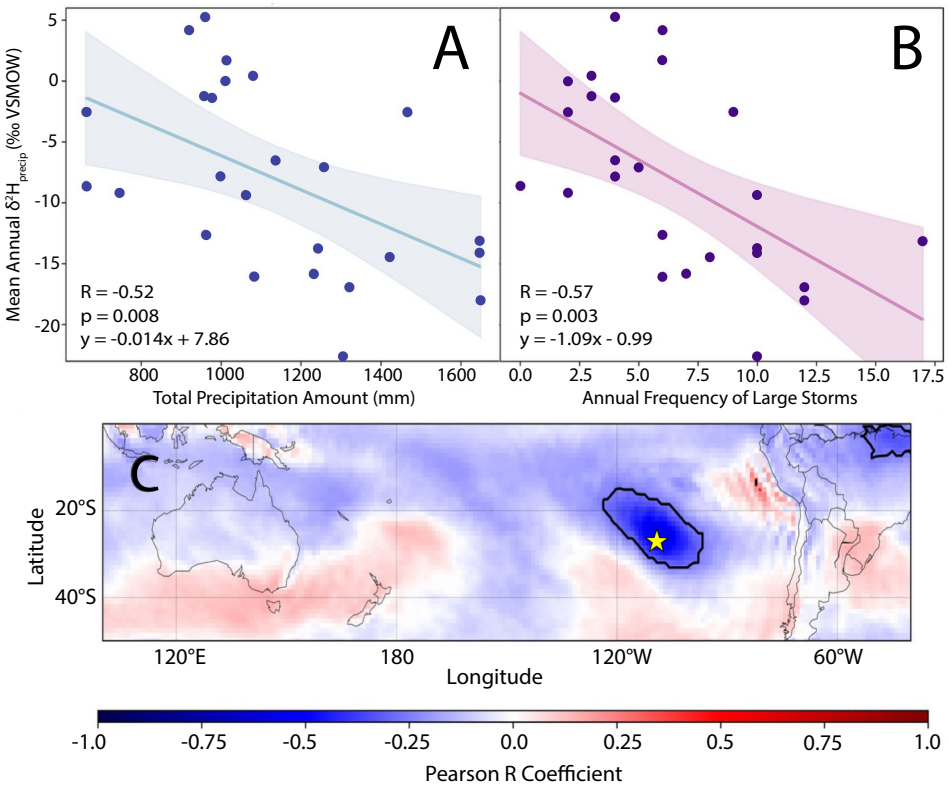

Fig. 2 | Isotopes in precipitation on Rapa Nui correlate with rainfall amount. A Annual precipitation amount and (**B**) annual frequency of large storms (>20 mm) compared with annual amount-weighted δ^2H_{precip} calculated from monthly data from the Global Network of Isotopes in Precipitation (GNIP) station on Rapa Nui. Years with <10 months of available δ^2H_{precip} data were excluded from the dataset. **C** Pearson regression coefficients for monthly ECHAM5-wiso simulated δ^2H_{precip} values over Rapa Nui (1871–2011) and the surrounding region (7° x 7° grid centered on Rapa Nui grid cell) compared against the simulated total precipitation values over the SH Pacific. Black contours represent a significance level of $p < 1e\text{-}24$. The location of Rapa Nui is starred.

plant growth is not seasonally restricted, we expect leaf waxes to record the mean annual δ^2H value of source water. Rano Kao is a rainwater-fed, closed-basin lake with no outflow. In Rano Kao, samples were extracted from a floating mat of totora (*Schoenoplectus californicus*), which sources water directly from the surrounding lake. Rano Kao lake water δ^2H values are determined by the hydrogen isotope composition of incoming precipitation (δ^2H_{precip}) and by evaporative fractionation. We expect these processes to be complementary. Intervals with fewer large storms would have more positive δ^2H_{precip} (see Equation 1) and greater evaporation would also result in more positive lake water δ^2H values. Plants in Rano Aroi on Terevaka peak (430 m) receive moisture from a combination of precipitation and groundwater[8]. Given that rainwater rapidly percolates through the subsurface on Rapa Nui, we anticipate relatively little post-depositional fractionation of hydrogen in rainwater during recharge of the main aquifer. This is supported by previous isotopic surveys (δ^2H, $\delta^{18}O$) on Rapa Nui, which show minimal offset between meteoric, borehole, and well water[8]. Thus, δ^2H_{wax} values in wetland plants likely reflect a multi-year integration of δ^2H_{precip} from groundwater, superimposed with higher frequency variability imparted from rainfall δ^2H_{precip}. We therefore interpret δ^2H_{wax} from Rano Aroi to represent δ^2H_{precip} and thereby precipitation amount on Rapa Nui (Equ. 1). We interpret δ^2H_{wax} from Rano Kao to reflect δ^2H_{precip}, compounded with the effect of evaporative fractionation on lake water.

δ^2H_{wax} values reveal onset of 16th century drought

In both the Rano Aroi and Rano Kao records, δ^2H_{wax} of C_{26} and C_{28} alkanoic acids show strong covariability (Fig. 3). δ^2H_{wax} values in Rano Kao are more positive than those in Rano Aroi, likely due to the evaporative fractionation of Rano Kao water and differences in altitude between the sites. At approximately 1200 CE in Rano Aroi, δ^2H_{wax} values began gradually decreasing, reaching a minimum at 1300 CE of −153.9‰ for C_{28} and −150.7‰ for C_{26}. From 1300-1850 CE, δ^2H_{wax} gradually increased by approximately 17‰ for C_{28} and 13‰ for C_{26}, showing the largest step change between 1500 and 1560 CE of 7.7‰ and 6.6‰ respectively. In the Rano Kao record, δ^2H_{wax} values reach a minimum later than in Rano Aroi, c. 1470 CE. Coincident with the positive δ^2H_{wax} excursions observed in Rano Aroi, δ^2H_{wax} values in Rano Kao sharply increased by 15–17‰ at approximately 1550 CE. Higher δ^2H_{wax} values persisted until the top of the Rano Kao sedimentary record, c. 1710 CE. We interpret the increase in δ^2H_{wax} at ~1550 CE in both records as an increase in δ^2H_{precip} over Rapa Nui, and thus a sustained decrease in regional precipitation.

To determine whether shifts in terrestrial vegetation on Rapa Nui (e.g. palm clearance) influenced the sources of *n*-alkanoic acids delivered to the Rano Aroi and Rano Kao, we calculated average chain lengths for long-chain (C_{26}-C_{32}) sedimentary *n*-alkanoic acids ($ACL_{26\text{-}32}$) (Methods). In Rano Aroi, $ACL_{26\text{-}32}$ shows virtually no change across the period of local palm deforestation (~1520–1620 CE) (Supplementary Fig. 5C)[47]. Additionally, carbon isotope measurements do not support a significant shift in C3/C4 plant distribution around Rano Aroi from at least ~1250 CE to European arrival[47]. In Rano Kao, there is similarly no change in $ACL_{26\text{-}32}$ across the interval of palm clearance (~1350–1800 CE)[48] (Supplementary Fig. 5C). Given the lack of stream inflow into the caldera and its steep, high walls, it is likely that long-chain leaf waxes in the floating mats of Rano Kao were produced almost entirely by wetland vegetation. For both sites, we therefore assume that leaf wax apparent fractionation ($\varepsilon_{wax\text{-}water}$) is constant prior to 1722 CE. We apply a $\varepsilon_{wax\text{-}water}$ value of −99‰, consistent with global averages[46,49].

There were dramatic ecological changes on Rapa Nui following Chilean annexation of Rapa Nui (1888 CE) due to the advent of intensive sheep farming on the island (1903-1953 CE) and the introduction of non-native plant species (e.g., *Eucalyptus*)[50,51]. $ACL_{26\text{-}32}$ values in Rano Aroi decrease significantly after 1890 CE, coinciding with an abrupt decrease in δ^2H_{wax} values (>20‰) and marked changes in sedimentology (Supplementary Fig. 6). For these reasons, we do not interpret δ^2H_{wax} values as a continuous proxy for precipitation after 1850 CE.

In Rano Aroi, mean δ^2H_{wax} values for the 1550–1720 CE period were 8.2‰ and 10.6‰ higher for C_{26} and C_{28} leaf-waxes, respectively, compared to the 1200–1550 CE period. This earlier interval broadly aligns with the timing of peak *ahu* construction on Rapa Nui, while the later interval

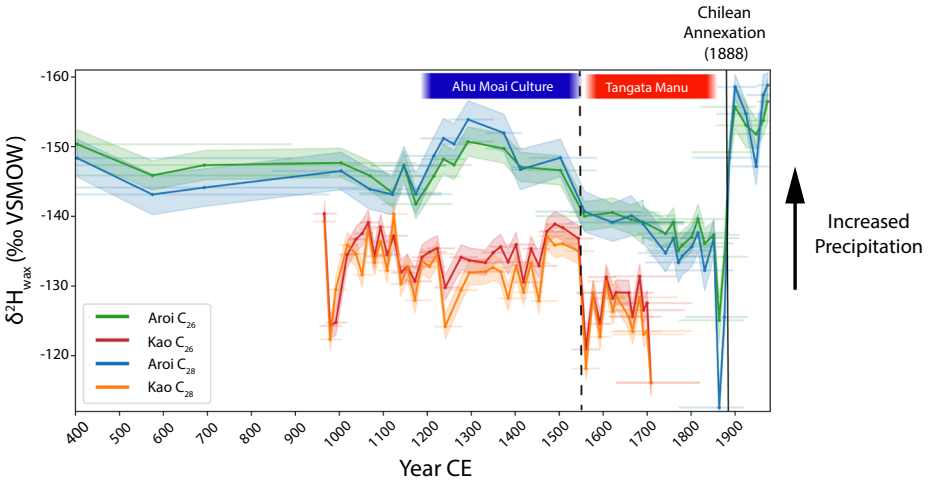

Fig. 3 | Leaf wax hydrogen isotopes in Rano Aroi and Rano Kao sediments. Leaf wax (*n*-alkanoic acid) hydrogen isotope values through time from Rano Aroi and Rano Kao. Results from C_{28} and C_{26} *n*-alkanoic acids are shown for both sites. Analytical precision in δ^2H_{wax} values is plotted as 1σ uncertainty based on pooled standard deviations of all replicates. The 95% confidence interval for the sample age is plotted, calculated using Bacon (Supplementary Fig. 8) for Rano Aroi and Clam R 2.2 for Rano Kao[22]. Note that the y-axis is inverted such that wetter conditions (more frequent large storms) are in the up direction.

overlaps with the emergence of *tangata manu*, prior to first European contact (1722 CE). Averaging these δ^2H_{wax} values for C_{26} and C_{28} alkanoic acids, the record suggests that δ^2H_{precip} values over Rapa Nui were ~10.4‰ higher from 1550 to 1720 CE relative to 1200-1550 CE, corresponding to a precipitation deficit of ~750 mm per year (Equation 1). In Rano Kao, mean δ^2H_{wax} values from 1550 to 1720 CE were 8.2‰ and 7.4‰ higher for C_{26} and C_{28} leaf waxes, respectively, compared to 1200 to 1550 CE. Applying Equation 1, we calculate a precipitation deficit of ~620 mm per year.

For context, a recent interval of drought on Rapa Nui (2010–2017), which put significant stress on local freshwater reserves and led to the drying of Rano Raraku[52], was associated with a mean reduction in annual precipitation of ~370 mm per year relative to the prior two decades in the Global Network of Isotopes in Precipitation dataset (Supplementary Fig. 7). A reduction in annual rainfall on the order of ~600–800 mm would have represented a significant shift in local hydroclimate and posed challenges to the Rapanui.

The timing of this inferred drought at ~1550 CE aligns with a hiatus in the Rano Raraku record (1550–1720 CE)[12], as well as geochemical indicators of sediment oxidation in Rano Aroi[38], both previously proposed to reflect drying. However, whereas there can be multiple, complex drivers of changes in wetland geochemistry and sediment accumulation rates, our record explicitly records paleoprecipitation variability on Rapa Nui and, based on model simulations, further suggests that drought was driven by a stronger South Pacific Anticyclone (Supplementary Fig. 4) that blocked approaching storm systems. It is challenging to attribute a strengthening and/or shift in SPA position during the 16th–18th century to a single cause, particularly given that the mean state of the tropical Pacific during this time period is not constrained. However, a strengthened SPA during the 16th–18th century is consistent with numerous proxy records of precipitation from South America, which indicate an enhanced summer monsoon[53–55]. Upper-level divergence associated with monsoonal heating over South America contributes to SPA strength by increasing subsidence to the west of the continent, leading to a region of high-pressure via the Rodwell-Hoskins mechanism[56].

Influence of drought on Rapanui society

There is evidence that the Rapanui dealt with freshwater scarcity from the time of their arrival. While crater lakes, and in particular Rano Kao, were likely relied upon for drinking water to some extent[57], recent studies suggest that coastal groundwater discharge was also a source of drinking water[9,58,59]. The locations of *ahu* are closely linked to coastal groundwater sources (Fig. 1), which enabled clans to disperse across the island[59]. The *ahu* themselves are thought to have delineated community control over these limited freshwater resources[59]. The Rapanui also engaged in a variety of freshwater management techniques, including rainwater harvesting in carved *taheta* basins and the construction of coastal cisterns known as *puna*[7,9,60,61]. Specialized agricultural techniques, such as lithic mulching, were employed to minimize evaporative moisture loss from soils, which are excessively drained[33,62].

Although the Rapanui were equipped to deal with limited freshwater resources and likely resilient to temporary reductions in rainfall, at approximately 1550 CE, a multi-century precipitation deficit led to the sustained drying of Rano Raraku lake and limited the amount of rainwater that could be collected in *taheta*. Initially, this drought may have pushed islanders to rely more heavily on coastal groundwater discharge, as theorized by Brosnan et al.[9]. Thermal imaging surveys conducted in 2019, following recent multi-year drought (2010–2018), indicated that while Rano Raraku and Rano Aroi quickly dried out, coastal groundwater discharge remained abundant due to the relatively long turnover time (10-50 years) of the island's main groundwater aquifer[8,9,58]. Importantly, however, the drought reconstructed here was more severe than that of recent years and persisted for well over a century. Therefore, it is plausible that after an initial phase of drought c. 1550 CE pushed islanders to more heavily rely on coastal groundwater discharge[9] a reduction in flow rate eventually reduced the potability of these waters for human consumption. Spatially inconsistent reductions in the coastal groundwater outflow, and thus water quality, further provides a plausible reason for changes in island geography – for example, the emergence of Rano Kao and its stable freshwater reservoir as an important hub of spiritual life on the island[25], or shifts in the importance of *ahu* as territorial signals at seep sites[59].

The paleohydroclimate records presented here suggest that freshwater availability had a role in shaping community geographies on Rapa Nui, perhaps due to the drying of Rano Raraku and Rano Aroi, the potability of water from coastal seeps, and the impact on agricultural yields following reductions in soil moisture. This scenario does not require increased clan warfare or demographic collapse, and instead provides a reasonable explanation for possible drivers of spatial reorganization, and an impetus for cultural changes on Rapa Nui.

Methods

Hydrogen isotopes of precipitation

The isotopic composition of hydrogen in precipitation is influenced by aspects of large-scale atmospheric dynamics and regional climate[44] and is expressed in delta notation relative to a standard (*Vienna Standard Mean Ocean Water*; VSMOW) according to the equation:

$$\delta^2H_{precip} = \left(\frac{^2H/H_{Sample}}{^2H/H_{VSMOW}} - 1\right) * 1000 \quad (2)$$

The δ^2H value of leaf waxes reflects the δ^2H value of plant source water[46]. In semiarid, subtropical climates that experience large, infrequent

rainfall events, large storms deliver precipitation that is relatively depleted in ^2H (i.e., with a more negative δ^2H value) and this isotopic signature is imparted into soil moisture[63]. Wetland sediments from Rapa Nui preserve an archive of leaf wax δ^2H values, thus recording regional hydroclimate variability through time. Here, we analyze two sediment cores: RAP-01-18 D1 from Rano Aroi wetland, and KAO08-03 from a floating mat of totora in Rano Kao.

Sample collection

Core KAO08-03 was collected from a floating mat in Rano Kao crater lake in 2008 using a Russian peat corer. The entire sequence of the mat was taken in five drives, extending to a depth of 300 cm[22]. Core RAP-01-18 was collected from Rano Aroi wetland in 2018 using a modified Nesje corer. Sediment was retrieved near the edge of the mire, close to the location of ARO 08 02, previously studied by Margalef et al.[64]. The entire core was taken in four drives and extends to ~420 cm. Only samples from Drive 1 (154 cm) are presented in this study. Sediments were refrigerated after collection and transported and stored in cold storage at the Lamont-Doherty Earth Observatory.

Quantifying *n*-Alkanoic Acid δ^2H_{wax} Values

Samples of 1 cm thickness were collected at 5 cm intervals from sediment core RAP-01-18 D1 from Rano Aroi mire, collected in 2018, and core KAO08-03. Additional sub-samples were taken across intervals with more rapid sediment accumulation, as determined by the ^{14}C-based age-depth models, to achieve consistent temporal sampling resolution where possible. Sediments were freeze dried and homogenized. Free lipids were extracted from each sample using a Dionex Accelerated Solvent Extractor (ASE 350) with a 9:1 v/v mixture of dichloromethane:methanol. Total lipid extracts (TLEs) were spiked with an internal standard mixture and split into an archive and a working half. The working sample was filtered over ashed glass wool to remove large particles, dried down under N_2 gas, and brought up in ~ 0.5 mL of 2:1 dichloromethane:isopropanol. To isolate neutral, acidic, and polar compounds respectively, TLEs were loaded onto a solvent-rinsed aminopropyl gel column and eluted with four bed volumes each of 2:1 dichloromethane:isopropanol, 4% acetic acid in ethyl ether, and methanol. The acid fraction containing *n*-alkanoic acids was then dried down, brought up in acetyl chloride-acidified methanol, and heated at 60 °C for 2 h in order to induce methylation. To track the isotopic composition of the added methyl group, a 100 uL sample of phthalic acid standard of a known isotopic composition (−95.5 ± 2.2‰) was methylated using the same procedure. Fatty acid methyl esters (FAMes) were then recovered from each sample using three liquid-liquid separations with 5:1 hexane:dichloromethane. FAMEs were further purified using silica gel chromatography, then transferred to 2 mL vials and brought up in ~500 uL of hexane for identification and quantification using Gas Chromatography Flame Ionization Detection (GC-FID) and compound-specific hydrogen isotope analysis using Gas Chromatography Isotope Ratio Mass Spectroscopy (GC-IRMS).

Hydrogen isotope compositions were run in triplicate for chain lengths C_{20}-C_{32} using a Trace GC-IRMS coupled to a Thermo DeltaV+ IRMS with ConFlo IV via GC Isolink. 1–3 uL of each sample was injected into a PTV inlet in splitless mode at 60 °C and rapidly heated to 320 °C before being vented onto the column using a helium (He) carrier gas. Oven temperature was held at 60 °C for 90 s, then ramped at 15 °C/min to 150 °C and again at 4 °C/min to 320 °C before being held for 10 minutes. Isotopic compositions were adjusted to the VSMOW scale and further corrected using the phthalic acid standard to account for the hydrogen isotope composition of the added methyl using the standard method described by Polissar & D'Andrea (2014)[65]. Samples with peak areas <10 Vs and >150 Vs were not used.

Quantifying *n*-alkanoic acid chain length distributions

C_{16}-C_{32} *n*-alkanoic acids were quantified using an Agilent 7890 gas chromatograph system with a flame ionization detector (GC-FID). 1–3 uL of each sample was injected into a multimode inlet in PTV mode at 60 °C, then rapidly heated to 320 °C and transferred onto the GC column using He gas. The oven was held at 60 °C for 90 seconds, ramped to 150 °C at 14 °C/min, then ramped at 4 °C/min to 320 °C and held for 25 minutes. Resulting flame ionization detector chromatogram peaks for each chain length were quantified by integration. Response factors for each chain length were calculated relative to C_{26} *n*-alkanoic acid using an external FAMe standard with known molecular concentrations, which was run every 5–6 samples. These response factors were then used to quantify chain-length abundance for sample *n*-alkanoic acids. Relative concentrations of each chain length were calculated by dividing the integrated ion response by the response factor.

Average chain-lengths were calculated across a variety of ranges (i = 20, 24, 26) using the following equation, where n indicates chain length, and C_n indicates chain length abundance:

$$ACL = \frac{\sum_i^{32}(C_n * n)}{\sum_i^{32}(C_n)} \quad (3)$$

$ACL_{26\text{-}32}$ is shown in Supplementary Fig. 5.

Isolation of terrestrial macrofossils and pollen extracts

To extract macrofossils, 1 cm-wide subsamples (5–8 ccs) were removed from the Rano Aroi sediment core using a clean spatula and filtered over a 125 µm sieve to remove clays and small organic particles. Terrestrial plant material (e.g., seeds, bark, leaves) was identified under a stereomicroscope and transferred to a 4 mL vial. Samples were then freeze dried and sent to the University of California Irvine Keck Facility for AMS C-14 dating. Pollen samples were extracted for parts of the sediment core with no identifiable terrestrial plant material in the >125 µm sieved fraction following a procedure modified from Vandergoes and Prior, 2003[66]. To generate pollen extracts, 5–8cc of sediment were boiled in 10% KOH solution for 10 min, then filtered through a 125 µm and 7 µm sieve using deionized (DI) water, discarding the fractions >125 µm and <7 µm. The sample was then centrifuged at ~3000 RPM for 10 min and the DI water decanted. A 10% HNO_3 solution was then added to each centrifuge tube and allowed to sit for 3-5 minutes to break up organic material. Samples were then centrifuged and decanted three times, rinsing with deionized water each time to remove any residual HNO_3. Density separations were performed using heavy liquid (polytungstate) with a density range of 1.2–1.35 SPT. Samples were rinsed once more with DI water, centrifuged, and transferred to 4 mL vials. A subset of samples were analyzed under 400x magnification to confirm the presence of pollen. Extracts were then freeze dried and sent for AMS C-14 dating at the UC Irvine Keck Facility.

Age modeling in BACON. An age model was constructed using the software Bacon[67]. Radiocarbon ages were converted to calendar age using the southern hemisphere SHcal20 calibration curve. For samples dated to the post-bomb period (1950 - present), $D^{14}C$ values were used to estimate a calendar age, using the CALIBomb software and the SH Zone 1–2 calibration dataset[68]. Priors including memory strength (4), memory mean (0.7), accumulation shape (2), and accumulation mean (135) were chosen in accordance with previous age models of Rano Aroi[64,69]. Sediment thickness was set to 4 cm, to allow for a slightly higher degree of smoothing relative to the default of 5 cm. Ages and associated errors from Rano Kao are taken from a published age model in Rull et al. (2018), which uses Clam.R 2.2 with smooth spline interpolation[22].

GNIP and ECHAM5-wiso analysis. Monthly measurements of hydrogen isotopes in precipitation over Rapa Nui ($n = 317$) were taken by the Global Network of Isotopes in Precipitation (GNIP) from 1991 to 2018[43]. These data were downloaded from GNIPs open-source, online database. For analysis of annual precipitation-weighted δ^2H_{precip} values, missing months in the dataset were ignored, and years with fewer than ten months of available δ^2H_{precip} data were excluded. Rho values, Pearson correlation coefficients, confidence intervals, and linear regressions between variables were calculated using the Scipy.stats package in Python.

Monthly ECHAM5-wiso model simulation data for the period 1871-2011 were downloaded from Zenodo repository associated with Steiger et al.[45]. Boundary conditions were interpolated HadISST fields. The model was run at 1 degree resolution. To investigate correlations between hydrogen isotopes in precipitation over Rapa Nui and regional climate variables, δ^2H_{precip} values and monthly precipitation amounts were extracted from a 7° x 7° grid, centered on Rapa Nui. A single δ^2H_{precip} value was calculated for the region as a precipitation amount-weighted mean of the individual grid cells. Pearson R correlation coefficients were calculated between these monthly δ^2H_{precip} values and total monthly precipitation amounts (Fig. 2C), 10 m wind speeds (Supplementary Fig. 4A), and sea level pressure (Supplementary Fig. 4B) for all other grid cells for the 1871–2011 time period, again using Scipy.stats.

Data availability

All new data presented in this study are available in the following, publicly accessible Dryad repository: [https://doi.org/10.5061/dryad.41ns1rnt2]. Monthly precipitation data from Rapa Nui were retrieved from the Water Isotope System for Electronic Retrieval (WISER) database, associated with the Global Network of Isotopes in Precipitation (GNIP). Storm frequency data associated with Steiger et al.[40] were provided by the authors upon request. ECHAM5-WISO datasets were sourced from the following Zenodo repository: https://zenodo.org/records/1249604.

Received: 31 March 2025; Accepted: 15 September 2025;
Published online: 05 November 2025

References

1. Zheng, J. et al. How climate change impacted the collapse of the Ming dynasty. *Climatic Change* **127**, 169–182 (2014).
2. Zhang, H. et al. Collapse of the Liangzhu and other Neolithic cultures in the lower Yangtze region in response to climate change. *Sci. Adv.* **7**, eabi9275 (2021).
3. Ren, M. et al. The collapse of the Ming Dynasty actually began with the Wanli megadrought: Insights from a hydroclimate reconstruction based on tree-ring $\delta^{18}O$ over the past 460 years. *Palaeogeogr., Palaeoclimatol., Palaeoecol.* **655**, 112548 (2024).
4. Cullen, H. M. et al. Climate change and the collapse of the Akkadian empire: Evidence from the deep sea. *Geology* **28**, 379–382 (2000).
5. deMenocal, P. B. Cultural Responses to Climate Change During the Late Holocene. *Science* **292**, 667–673 (2001).
6. Hodell, D. A., Curtis, J. H. & Brenner, M. Possible role of climate in the collapse of Classic Maya civilization. *Nature* **375**, 391–394 (1995).
7. Hixon, S. W., DiNapoli, R. J., Lipo, C. P. & Hunt, T. L. The Ethnohistory of Freshwater Use on Rapa Nui (Easter Island, Chile). *J. Polynesian Soc.* **128**, 163–190 (2019).
8. Herrera, C. & Custodio, E. Conceptual hydrogeological model of volcanic Easter Island (Chile) after chemical and isotopic surveys. *Hydrogeol. J.* **16**, 1329–1348 (2008).
9. Brosnan, T., Becker, M. & Lipo, C. Coastal groundwater discharge and the ancient inhabitants of Rapa Nui (Easter Island), Chile. *Hydrogeol. J.* **27**, 519–534 (2018).
10. Bradley, R. S., D'Andrea, W. J., Diaz, H. F. & Ning, L. Climatology of Rapa Nui (Isla de Pascua, Easter Island). in *The Prehistory of Rapa Nui (Easter Island): Towards an Integrative Interdisciplinary Framework* (eds. Rull, V. & Stevenson, C.) 259–274 (Springer International Publishing, Cham, 2022). https://doi.org/10.1007/978-3-030-91127-0_11.
11. Mann, D. et al. Drought, vegetation change, and human history on Rapa Nui (Isla de Pascua, Easter Island). *Quat. Res.* **69**, 16–28 (2008).
12. Cañellas-Boltà, N. et al. Vegetation changes and human settlement of Easter Island during the last millennia: a multiproxy study of the Lake Raraku sediments. *Quat. Sci. Rev.* **72**, 36–48 (2013).
13. Schmid, M. M. E. et al. How 14C dates on wood charcoal increase precision when dating colonization: The examples of Iceland and Polynesia. *Quat. Geochronol.* **48**, 64–71 (2018).
14. DiNapoli, R. J., Rieth, T. M., Lipo, C. P. & Hunt, T. L. A model-based approach to the tempo of "collapse": The case of Rapa Nui (Easter Island). *J. Archaeological Sci.* **116**, 105094 (2020).
15. Hunt, T. L. & Lipo, C. P. Late Colonization of Easter Island. *Science* **311**, 1603–1606 (2006).
16. Wilmshurst, J. M., Hunt, T. L., Lipo, C. P. & Anderson, A. J. High-precision radiocarbon dating shows recent and rapid initial human colonization of East Polynesia. *Proc. Natl. Acad. Sci.* **108**, 1815–1820 (2011).
17. Martinsson-Wallin, H., Wallin, P., Anderson, A. & Solsvik, R. Chronogeographic Variation in Initial East Polynesian Construction of Monumental Ceremonial Sites. *J. Isl. Coast. Archaeol.* **8**, 405–421 (2013).
18. Van Tilburg, J. Easter Island. in *Encyclopedia of Prehistory* 45–59 (Springer, Boston, MA, 2001). https://doi.org/10.1007/978-1-4615-1189-2_8.
19. Richards, C. et al. Road my body goes: re-creating ancestors from stone at the great moai quarry of Rano Raraku, Rapa Nui (Easter Island). *World Archaeol.* **43**, 191–210 (2011).
20. Flenley, J. & Bahn, P. G. The Enigmas of Easter Island: Island on the Edge. *Oxford University Press*. (2002)
21. Edwards E. et al. When the Universe was an island: exploring the cultural and spiritual Cosmos of Ancient Rapa Nui. *Hangaroa: Hangaroa Press* (2013).
22. Rull, V. et al. CLAFS, a Holistic Climatic-Ecological-Anthropogenic Hypothesis on Easter Island's Deforestation and Cultural Change: Proposals and Testing Prospects. *Front. Ecol. Evol.* **6**, 1–12 (2018).
23. Robinson, T. & Stevenson, C. M. The Cult of the Birdman: Religious Change at 'Orongo, Rapa Nui (Easter Island). *J. Pac. Archaeol.* **8**, 88–102 (2017).
24. Lee, G. & Liller, W. Easter Island's "Sun Stones": A Re-Evaluation. *J. Hist. Astron.* **18**, S1–S11 (1987).
25. Rull, V. Natural and anthropogenic drivers of cultural change on Easter Island: Review and new insights. *Quat. Sci. Rev.* **150**, 31–41 (2016).
26. Kirch, P. V. *On the Road of the Winds: An Archaeological History of the Pacific Islands Before European Contact, Revised and Expanded Edition*. (Univ of California Press, 2017).
27. Mulrooney, M., Van Tilburg, J., Hom, A. & McCoy, P. C. Refining the Chronology of Rapa Nui (Easter Island) Settlement: the Re-dating of Residential Sites on the Eastern Rim of Rano Kau. *J. Pacific Archaeol.* 72–83, https://doi.org/10.70460/jpa.v12i1.318 (2021).
28. Seco, I. et al. A Continuous Palynological Record of Forest Clearing at Rano Kao (Easter Island, SE Pacific) During the Last Millennium: Preliminary Report. *Quaternary* **2**, 22 (2019).
29. Stevenson, C. M. et al. Variation in Rapa Nui (Easter Island) land use indicates production and population peaks prior to European contact. *Proc. Natl. Acad. Sci.* **112**, 1025–1030 (2015).
30. Stevenson, C. M., Ladefoged, T. N. & Chadwick, O. Prehistoric settlement, ancient gardens and population dynamics on the Hiva Hiva lava flow, Rapa Nui, Chile. in *Cultural and Environmental Change on Rapa Nui* (Routledge, 2017).
31. Stevenson, C. M., Archaeological Investigations on Easter Island: Maunga Tari: An Upland Agricultural Complex. Los Osos, CA: *Bearsville Press and Cloud Mountain Press* (1997).
32. Moreno-Mayar, J. V. et al. Ancient Rapanui genomes reveal resilience and pre-European contact with the Americas. *Nature* **633**, 389–397 (2024).
33. Davis, D. S., DiNapoli, R. J., Pakarati, G., Hunt, T. L. & Lipo, C. P. Island-wide characterization of agricultural production challenges the demographic collapse hypothesis for Rapa Nui (Easter Island). *Sci. Adv.* **10**, eado1459 (2024).
34. Boersema, J. J. The Human Giants of Easter Island (Rapa Nui). in *The Prehistory of Rapa Nui (Easter Island): Towards an Integrative Interdisciplinary Framework* (eds. Rull, V. & Stevenson, C.) 589–607 (Springer International Publishing, Cham, 2022). https://doi.org/10.1007/978-3-030-91127-0_23.

35. Mulrooney, M. A. An island-wide assessment of the chronology of settlement and land use on Rapa Nui (Easter Island) based on radiocarbon data. *J. Archaeological Sci.* **40**, 4377–4399 (2013).
36. Peiser, B. From Genocide to Ecocide: The Rape of Rapa Nui. *Energy Environ.* **16**, 513–539 (2005).
37. Diamond, J. Collapse: How Societies Choose to Fail or Succeed: Revised Edition. (Penguin Books, New York, 2011).
38. Roman, M. et al. A multi-decadal geochemical record from Rano Aroi (Easter Island/Rapa Nui): Implications for the environment, climate and humans during the last two millennia. *Quat. Sci. Rev.* **268**, 107115 (2021).
39. Rull, V. & Stevenson, C. *The Prehistory of Rapa Nui (Easter Island): Towards an Integrative Interdisciplinary Framework*. (Springer Nature, 2022).
40. Steiger, N. J., D'Andrea, W. J., Smerdon, J. E. & Bradley, R. S. Large infrequent rain events dominate the hydroclimate of Rapa Nui (Easter Island). *Clim. Dyn.* **59**, 595–608 (2022).
41. Seager, R. et al. Air–Sea Interaction and the Seasonal Cycle of the Subtropical Anticyclones. *J. Clim.* **16**, 1948–1966 (2003).
42. Delcroix, T. et al. Clarifying the Role of ENSO on Easter Island Precipitation Changes: Potential Environmental Implications for the Last Millennium. *Paleoceanogr. Paleoclimatology* **37**, e2022PA004514 (2022).
43. IAEA/WMO (2024). Global Network of Isotopes in Precipitation. The GNIP Database. Accessible at: https://nucleus.iaea.org/wiser
44. Sharp, Z. Principles of Stable Isotope Geochemistry, 2nd Edition. *Open Textbooks* (2017) https://doi.org/10.25844/h9q1-0p82.
45. Steiger, N. J., Steig, E. J., Dee, S. G., Roe, G. H. & Hakim, G. J. Climate reconstruction using data assimilation of water isotope ratios from ice cores. *J. Geophys. Res.: Atmospheres* **122**, 1545–1568 (2017).
46. Hou, J., D'Andrea, W. J. & Huang, Y. Can sedimentary leaf waxes record *D/H* ratios of continental precipitation? Field, model, and experimental assessments. *Geochimica et. Cosmochimica Acta* **72**, 3503–3517 (2008).
47. Rull, V. et al. Late Holocene vegetation dynamics and deforestation in Rano Aroi: Implications for Easter Island's ecological and cultural history. *Quat. Sci. Rev.* **126**, 219–226 (2015).
48. Butler, K. R. & Flenley, J. R. The Rano Kau 2 Pollen Diagram: Palaeoecology Revealed. *Rapa Nui J.* **24**, 5–10 (2010).
49. McFarlin, J. M., Axford, Y., Masterson, A. L. & Osburn, M. R. Calibration of modern sedimentary δ^2H plant wax-water relationships in Greenland lakes. *Quat. Sci. Rev.* **225**, 105978 (2019).
50. Jackson-Stepowski, S. & Gabon-Bautista, A. The Easter island sheep farm cultural landscape. *Historic Environ.* **31**, 28–39 (2021).
51. Porteous, J. D. Easter Island: The Scottish Connection. *Geographical Rev.* **68**, 145–156 (1978).
52. Giraldo, M. Chill waters, arid land: climate change arrives on Easter Island. *Reuters* (2019).
53. Thompson, L. G., Mosley-Thompson, E., Dansgaard, W. & Grootes, P. M. The Little Ice Age as Recorded in the Stratigraphy of the Tropical Quelccaya Ice Cap. *Science* **234**, 361–364 (1986).
54. Reuter, J. et al. A new perspective on the hydroclimate variability in northern South America during the Little Ice Age. *Geophys. Res. Lett.* **36**, L21706 (2009).
55. Bernal, J. P. et al. High-resolution Holocene South American monsoon history recorded by a speleothem from Botuverá Cave, Brazil. *Earth Planet. Sci. Lett.* **450**, 186–196 (2016).
56. Rodwell, M. J. & Hoskins, B. J. Subtropical Anticyclones and Summer Monsoons. *J. Clim.* **14**, 3192–3211 (2001).
57. Rull, V. Drought, freshwater availability and cultural resilience on Easter Island (SE Pacific) during the Little Ice Age. *Holocene* **30**, 774–780 (2020).
58. DiNapoli, R. J., Lipo, C. P., de Smet, T. S. & Hunt, T. L. Thermal Imaging Shows Submarine Groundwater Discharge Plumes Associated with Ancient Settlements on Rapa Nui (Easter Island, Chile). *Remote Sens.* **13**, 2531 (2021).
59. DiNapoli, R. J. et al. Rapa Nui (Easter Island) monument (ahu) locations explained by freshwater sources. *PLOS ONE* **14**, e0210409 (2019).
60. Morrison, A. E. An archaeological analysis of Rapa Nui settlement structure: A multi-scalar approach. (University of Hawai'i at Manoa, United States -- Hawaii) (2012).
61. Métraux, A. Easter Island; a Stone-Age Civilization of the Pacific. New York: Oxford University Press. (1957).
62. Wozniak, J. A. Prehistoric Horticultural Practices on Easter Island: Lithic Mulched Gardens and Field Systems. *Rapa Nui J.* **13**, 95–99 (1999).
63. Skrzypek, G., Dogramaci, S., Page, G. F. M., Rouillard, A. & Grierson, P. F. Unique stable isotope signatures of large cyclonic events as a tracer of soil moisture dynamics in the semiarid subtropics. *J. Hydrol.* **578**, 124124 (2019).
64. Margalef, O. et al. A 70,000 year multiproxy record of climatic and environmental change from Rano Aroi peatland (Easter Island). *Glob. Planet. Change* **108**, 72–84 (2013).
65. Polissar & D'Andrea, P. J. W. J. Uncertainty in paleohydrologic reconstructions from molecular δD values. *Geochimica et. Cosmochimica Acta* **129**, 146–156 (2014).
66. Vandergoes, M. J. & Prior, C. A. AMS Dating of Pollen Concentrates—A Methodological Study of Late Quaternary Sediments from South Westland, New Zealand. *Radiocarbon* **45**, 479–491 (2003).
67. Blaauw, M. & Christen, J. A. Flexible paleoclimate age-depth models using an autoregressive gamma process. *Bayesian Anal.* **6**, 457–474 (2011).
68. Reimer, R. W. & Reimer, P. J. 2025CALIBomb [WWW program] at http://calib.org accessed 2025
69. Horrocks, M. et al. A plant microfossil record of Late Quaternary environments and human activity from Rano Aroi and surroundings, Easter Island. *J. Paleolimnol.* **54**, 279–303 (2015).

Acknowledgements

We would like to thank the Ma'u Henua Indigenous Community and the Chilean National Forestry Service (CONAF) for permitting and logistically supporting field work on Rapa Nui conducted for this study, as well as the Rapa Nui Office of the Secretaría Técnica de Patrimonio at the Consejo de Monumentos Nacionales for permission to excavate and export sediment cores. Excavation permit was granted under permit 6214 (27-12. 2017) and permission to export sediment cores to the USA under permit 2869 (04.07.2018). We would like to acknowledge the support of the National Science Foundation award EAR-1903676 to WJD and the William & Mary Reves Faculty Fellowship to NLB. We additionally thank the Vetlesen Foundation and Explorer's Club for funding provided to WJD and LC respectively. We recognize additional contributions from Project GEOBILA (CGL2007-60932/BTE), provided by the Spanish Ministry of Education and Science. We thank Helen Habicht, Wei Huang, Sachi Thomson, and Tyler Clemens for their assistance in the lab, and James Van Hook, Nicolás Pakomio, Arone Rapu, and Dionisio (Peter) Teao for their assistance with field work.

Author contributions

W.J.D. conceived of the study project and oversaw activities relating to research, including field work, lab work, and writing. R.S. conducted laboratory work, data analysis, and wrote the manuscript. R.S.B. helped conceive of this project, and N.L.B., L.C., and R.S.B. conducted field work and contributed to writing the manuscript. N.L.B. also contributed to laboratory work. D.M.P. provided laboratory facilities and oversight of macrofossil identification, assisted with pollen extraction for the Rano Aroi age model, and edited the manuscript. V.R. provided sediment for the Rano Kao record and contributed to writing the manuscript. R.R. and A.S. oversaw field work on Rapa Nui and provided guidance on archeological

interpretations, and A.S contributed to writing the manuscript. Correspondence should be addressed to R.S and W.J.D.

Competing interests
The authors declare no competing interests.

Additional information
Supplementary information The online version contains supplementary material available at https://doi.org/10.1038/s43247-025-02801-4.

Correspondence and requests for materials should be addressed to Redmond Stein or William J. D'Andrea.

Peer review information *Communications Earth & Environment* thanks the anonymous reviewers for their contribution to the peer review of this work. Primary Handling Editors: Soumaya Belmecheri, Aliénor Lavergne, and Martina Grecequet. A peer review file is available.